DOI 10.31489/2021PH4/25-34

UDC 539.013

V.M. Yurov[1*], V.I. Goncharenko[2,3], V.S. Oleshko[2], K.M. Makhanov[1]

[1]Karaganda University of the name of academician E.A. Buketov, Kazakhstan;
[2]Moscow Aviation Institute (National Research University), Moscow, Russia;
[3]Institute for Management Problems. V.A. Trapeznikov RAS, Moscow, Russia
([*]e-mail: exciton@list.ru)

Anisotropy of the surface energy of silicides of some metals

An empirical model of a solid surface is proposed in the article. The thickness of the surface layer is described in terms of one parameter – the atomic volume of an element or its compounds. Surface energy is also expressed through one parameter – the melting point of a chemical element or crystal. The model proposes equations that allow calculating the thickness of the surface layer and surface energy for each face of the crystal. As an example, calculations of these values are made for silicides of some metals with crystal structures of cubic, hexagonal and rhombic systems. For cubic silicides, the thickness of the surface layer is 3-9 nm, and the number of monolayers is 7-16. Studies of metal deposition on silicon faces have shown that silicon silicide is formed on the (111) face, which has the highest surface energy. The reaction on the (100) face occurs only on the oxidized surface. In hexagonal silicides, anisotropy is seen, both in the values of the thickness of the surface layer and in the values of the surface energy. For example, during the formation of chromium disilicide on the (111) face in the *c* direction, it was found that the sizes of the islands become larger than on the (001) face. The authors designate that the thickness of the surface layer and the specific surface energy for cubic, hexagonal, and rhombic crystals significantly differ from them. What is the difference? First, the difference between the atoms of chemical elements from the periodic table and their compounds depends, first of all, on their electronic structure, which forms this or that interaction potential. Secondly, the difference between cubic, hexagonal and rhombic crystals lies in their relationship with Poisson's ratio and Young's modulus, that is, on two material parameters. Third, the thickness of the surface layer between cubic, hexagonal, and rhombic crystals also differs in only one parameter – the atomic (molar) volume of the crystal. However, the analysis of all the patterns still needs to be carefully analyzed.

Keywords: metal silicide, surface energy, thickness of the surface layer, solid, chemical element, crystal, surface layer, Poisson's ratio, Young's modulus.

Introduction

Silicides are compounds that are similar to metals. They have a good electrical conductivity, thermal conductivity and even superconductivity at low temperatures. Silicides in the silicon-metal system do not have a simple chemical bond in the structure of interstitial phases and do not fulfill the Hagg relation [1]. Due to the significant radius of silicon atoms, its high solubility by transition metals in structures and solid solutions is observed by the type of substitution. In metals with significant atomic radii, complex silicide structures are formed with a prevailing covalent bond of silicon atoms. With the transition of metals to groups VII and VIII, the structures of silicides become simpler. Disilicides of metals such as tantalum, zirconium, vanadium, chromium, niobium silicon form layered structures as curved nets. In the formation of silicides from transition metals, the decisive role is played by covalent bonds, which resonate between the electronic states of the s and d orbitals. The fact that the d-orbitals are empty leads to a large number of observed silicide structures.

When silicon forms solid solutions, its atom is transformed into +4 ion due to ionization. Such a solid solution has orthogonal symmetry and creates body-centered (bcs) structures with many metals from the periodic table.

Transition metal silicides are relevant today in microelectronics and nanoelectronics because of their low electrical resistivity and high melting temperature. Contacts for integrated circuits, thin thermal stable film connections, Schottky diodes and more. All this dictates the relevance of studies of diffusion processes in metal-silicon systems and the conditions for the formation of metal silicides [2]. Transition metal silicides have thermal and mechanical strength, which decreases when going from titanium to tungsten.

During the deposition of a metal coating on silicon at its initial stage, silicides of different chemical composition, different structural composition and intermediate phases can be formed at the interface. It all depends on the type of metal applied, its characteristics, temperature, and other thermodynamic parameters, crystallization kinetics, and much more.

Metal-silicon structures, which are widely used in microelectronics for soft X-ray radiation, contain a layer thickness in the nanoscale range. Therefore, it is believed that the nanometer thickness of metal silicides will provide the key to understanding many processes.

In this work, based on an empirical model, we present the values of the thickness of the surface layer of silicides, which can be experimentally determined by the methods of “grazing” X-rays [2], as well as the anisotropy of the surface energy for various faces, which was determined by us for the first time.

The difference in the radii of the metal and silicon atoms leads to a significant difference in their diffusion, which is determined by the activation energy, which, in turn, depends on the specific energy for each silicon face. This means that in order to understand the processes occurring during the formation of silicides either due to metal diffusion or due to its crystallization, it is necessary to know the specific surface energy and its anisotropy for silicides of some metals.

With regard to surface energy, we present several recent works that have been performed theoretically. In work [3], the surface characteristics of some metals were obtained using the traditional method of electron density, but using new test functions at the vacuum-metal interface. This method gave good agreement with the anisotropic behavior of some metals.

In work [4], the anisotropy of the metal in the s-surface layer was estimated by the electronic statistical method. In this case, considering the dispersion forces on the edges of the metal, the theory of E.M. Lifshitz calculates the attraction of molecules in the condensed phase and allows to determine the interaction energy through the constants of a solid.

In [5], a method was proposed for determining a layer thickness on the surface of a crystal that melts at the melting temperature. In this case, the thickness means the first coordination sphere of atoms, which is perpendicular to the surface. It facilitates to estimate the anisotropy of the surface energy of metals. In the same work, a model of the coordination melting of a solid was proposed, which made it possible to relate the surface energy to the physical properties of the crystal.

Experimental

Five silicides V_3Si, *FeSi, CoSi, MnSi*, Mg_2Si, which have a cubic crystal lattice, were selected as objects of study.

Trivanadium silicide V_3Si is produced by condensation of silicon and vanadium vapors in vacuum. In this case, gray crystals of a cubic system are formed with a superconductivity temperature of about 17.2 K. It can be used in magnetic devices in electrical engineering.

Iron silicide *ε-FeSi* forms yellow cubic crystals. It is part of ferrosilicon, which is used in the deoxidation of all steels. It is used for alloying structural and transformer steel grades. In [6], the formation of iron silicide on the silicon (100) and (111) faces was studied, similarly to how it was shown in [2]. It turned out that if iron is deposited on the (111) face, then it immediately interacts with this face, forming an *ε-FeSi* silicide of the cubic system. However, on the (100) face, iron first forms a solid solution, which passes into the *Fe3Si* phase.

Cobalt silicide *CoSi* is obtained from the solid phase with copper silicide at a temperature of 1500 °C. These are gray crystals of a cubic system. In [7], the formation of silicides upon the deposition of cobalt was studied on the silicon faces (100), (110) and (111). When a cobalt film less than 0.7 nm is applied, a cobalt silicide layer of about 0.17 nm is formed. Upon annealing a nanometer-thick substrate above 300 ºC, four silicide phases arise – nonmagnetic *CoSi*, Co_2Si, $CoSi_2$, and ferromagnetic Co_3Si.

Manganese silicide *MnSi* has a gray cubic crystal, the lattice of which does not contain inversion symmetry. In other words, its unit cell is not combined with itself by mirror reflection, and at low temperatures skyrmions are formed, first discovered by German physicists in 2009 [8]. Skyrmions have a nonzero topological charge (N = 1) and are highly localized (magnetic skyrmions are 50-100 nm in size). In [9], the initial stage of growth of manganese films on the (100) and (111) silicon faces at room temperature was studied. When 0.6 nm of manganese is deposited, a 0.1 nm thick monosilicide layer is formed. Upon annealing a silicon crystal, on the face of which 2.5 nm manganese was deposited, manganese monosilicide and a *Mn-Si* solid solution were formed. The formation of these silicide films took place at temperatures of 200-400 ºC. When manganese silicide is heated above 600 ºC, it turns into semiconducting silicide $MnSi_{17}$.

Magnesium silicide Mg_2Si is a blue crystal of a cubic system and a semiconductor material with a band gap of 0.76 eV. It is used as heat-to-electricity converters in silicon technology. In [10], the deposition of coatings on the (111) face was investigated at a magnesium deposition rate of about 0.06 nm / min. In this case, three stages of the formation of coatings appeared at the interface. The first stage is the formation of clusters of magnesium atoms. In the second stage, magnesium silicide increases. The third stage illustrates the growth of metallic magnesium.

Five silicides Ti_5Si_3, $NbSi_2$, $TaSi_2$, $CrSi_2$, $MoSi_2$, which have a crystal lattice of hexagonal syngony. Titanium silicide Ti_5Si_3 is a hexagonal structure and has a high melting point, which makes it a heat-resistant material [11].

Niobium silicide (disilicide) $NbSi_2$ forms crystals of a hexagonal system. The metal sublattice has a hexagonal closest packing, and six octahedral voids are occupied by silicon atoms and their arrangement is ordered. The structure is constructed, so that the niobium atom contains six silicon atoms, which are surrounded by three niobium atoms ($NbSi_2$). The $NbSi_2$ structure is located between silicides with silicon chains and layers of silicon atoms. In [12], the formation of $NbSi_2$ disilicide is established during the diffusion of silicon through the interface during electron beam evaporation to the silicon (111) face in vacuum. The thickness of the layer depends on the temperature during bombardment of the target with argon ions, which turned out to be maximum at T = 773 K. The absence of the influence of the energy of argon ions on the diffusion of niobium into flint suggests that radiation does not affect the formation of niobium silicides.

Tantalum silicide (disilicide) $TaSi_2$ forms crystals of a hexagonal system. It has metallic conductivity, while silicon has no free electrons in the $TaSi_2$ silicide. This leads to the appearance of a polarization dipole moment. Tantalum silicide has a high melting point (2200 ºC), low electrical resistance, high modulus of elasticity. It is used in Schottky barriers, ohmic contacts of integrated circuits. The interaction of conducting tantalum disilicide $TaSi_2$ with semiconducting silicon Si leads to the formation of Janus-like nanoparticles $TaSi_2/Si$ [13].

Chromium silicide (disilicide) $CrSi_2$ has a hexagonal structure with three chromium atoms in a unit cell and 6 silicon atoms. Chromium disilicide $CrSi_2$ is an indirect-gap semiconductor with a band width of 0.35 eV at points *L* and *M*. At point *L*, there is a gap with a band width of 0.52 eV. In [14], chromium films 30 nm thick were deposited on the silicon (111) face by magnetron sputtering in a vacuum setup. The formation of a $CrSi_2$ layer at a temperature of about 400 ºC, which has a resistivity of about 1.2 mΩ x cm and a Schottky barrier height of about 0.6 V.

Molybdenum silicide (disilicide) $MoSi_2$ contains a tetragonal structure. Each unit cell contains 2 molybdenum atoms and 4 silicon atoms. Along the z axis, a change of double dense layers of silicon atoms with layers of molybdenum atoms is observed. In other words, silicon atoms form a structure in the voids of which molybdenum atoms are located. Molybdenum disilicide $MoSi_2$ has two polymorphic modifications – α-*MoSi2* has a tetragonal structure and β-$MoSi_2$ has a hexagonal structure. The hexagonal structure is a metastable phase, while the tetragonal structure, on the contrary, is a stable phase [15], as evidenced by the fact that the bond between molybdenum and silicon atoms is much stronger than between *Si - Si* atoms.

Five silicides $ZrSi_2$, $HfSi_2$, $FeSi_2$, Co_2Si, Ni_2Si, which have a rhombic crystal lattice, were selected as the third objects of study.

Zirconium silicide (disilicide) $ZrSi_2$ forms rhombic crystals. In [16], the zirconium coating on the (100) face of silicon was investigated when the latter was irradiated with an electron beam with a density of 8-10 J/cm^2. Zirconium disilicide $ZrSi_2$ with a size of 40-50 nm is formed at the interface.

Hafnium silicide (disilicide) *HfSi2* is a substance of the rhombic system. It is obtained by spraying pure hafnium with a magnetron or laser onto silicon. The quality of silicon silicide *HfSi2* is investigated experimentally.

Iron silicide (disilicide) $FeSi_2$ is a β-$FeSi_2$ crystal of rhombic system. The quality of semiconductor iron disilicide depends on the material purity and the level of defects present. Electron beam evaporation of β-$FeSi_2$ shows better results than magnetron coating. The band diagram of β-$FeSi_2$ illustrates a direct transition at 0.74 eV at the *Λ* point, which is in the middle between the *Γ-Z* points [17].

Dicobalt silicide Co_2Si forms gray rhombic crystals. It was established in [18] that the hydrogen evolution reaction on the dicobalt Co_2Si electrode proceeds according to the Langmuir type.

Dinickel silicide Ni_2Si is a white rhombic crystal.

In [19], we showed that the thickness $R(I)_M$ of the surface layer of an atomically smooth crystal can be estimated by the formula:

$$R(I)_i = 0.24 \cdot 10^{-9} \cdot \upsilon(\mathrm{nm}), \tag{1}$$

where the molar (atomic) volume of the crystal υ = M/ρ, M is the molar (atomic) mass (g/mol), ρ is the density (g/cm^3) of the crystal. These values are given in the periodic table and in many reference books.

For example, for silicon Si, the molar mass is M = 28.086 (g/mol), the density is ρ = 2.33 (g/cm^3), then $R(I)_M$ = 2.9 nm. The experimental value of the silicon layer thickness measured by the method of grazing X-rays is 3.1 nm, which does not differ from our value with the experimental error. With formula (1), $R(I)_M$ of all elements of the periodic system can be calculated. It turned out that this value does not exceed 5-7 nm, that is, all the elements of the periodic system are nanostructure. As for silicon, its crystal lattice constant is a = 0.54307 nm. This means that on the thickness of silicon $R(I)_M$ there are monolayers in the amount of $n = R(I)_M/a \approx 6$. In other words, silicon is reconstructed on these 6 monolayers, which was discovered experimentally.

According to the empirical model [19] for the surface energy σ of the crystal face, we obtained:

$$\sigma(\mathrm{hkl}) = 10^{-3} \cdot T_{\mathrm{m}} \cdot \mathrm{l(hkl)}, \tag{2}$$

where Tm is the melting point of the crystal, and l *(hkl)* for crystals with body-centered (bcc) and face-centered (fcc) cubic structures is given by relations (3):

$$\begin{aligned} &\mathrm{Im3m,\ Z = 2;\ l_{100} = a;\ l_{110} = a\sqrt{2};\ l_{111} = a/\sqrt{3},} \\ &\mathrm{Fd3m,\ Z = 4;\ l_{100} = a;\ l_{110} - a/\sqrt{2};\ l_{111} = 2a/\sqrt{3}.} \end{aligned} \tag{3}$$

It is necessary to write equations (1) and (2), taking into account the anisotropy of crystals, the directions of the crystal faces. Let us write them out finally:

$$\begin{aligned} \mathrm{R(I)_{x=a}} &= 0.54 \cdot 10^{-11} \cdot \mathrm{x(a)^3}, \\ \mathrm{R(I)_{y=b}} &= 0.54 \cdot 10^{-11} \cdot \mathrm{y(b)^3}, \\ \mathrm{R(I)_{z=c}} &= 0.54 \cdot 10^{-11} \cdot \mathrm{z(c)^3}. \end{aligned} \tag{4}$$

$$\begin{aligned} \sigma_a &= 10^{-3} \cdot \mathrm{T_m} \cdot \mathrm{R_a(I)/R(I)} \\ \sigma_b &= 10^{-3} \cdot \mathrm{T_m} \cdot \mathrm{R_b(I)/R(I)} \\ \sigma_c &= 10^{-3} \cdot \mathrm{T_m} \cdot \mathrm{R_c(I)/R(I).} \end{aligned} \tag{5}$$

Results and Discussion

We will consider the thickness of the surface layer and the surface energy of silicides of the cubic, hexagonal, rhombic systems and compare them. Table 1 demonstrates 5 silicides having a cubic structure. The thickness of the surface layer for cubic filicides is 3-9 nm, and the number of monolayers is 7-16. For monosilicides it is equal to 7. These *FeSi, CoSi, MnSi* crystals have a structure of reduced dimensionality of the skyrmion type [8], in which the crystal lattice does not contain inversion symmetry (Fig. 1).

Table 2

Thickness of the surface layer and anisotropy of the surface energy of silicides cubic system

Compound	(hkl)	Syngonia	T_m, K	$R(I)_M$, nm	σ_{hkl}, μJ/m^2
V_3Si	100	Cubic	2003	7.6 (16)	2.003
	110				1.431
	111				2.289
FeSi	100	Cubic	1678	3.2 (7)	1.678
	110				1.199
	111				1.918
CoSi	100	Cubic	1600	3.3 (7)	1.600
	110				1.143
	111				1.829
MnSi	100	Cubic	1548	3.4 (7)	1.548
	110				1.106
	111				1.769
Mg_2Si	100	Cubic	1358	9.5 (15)	1.358
	110				0.970
	111				1.552

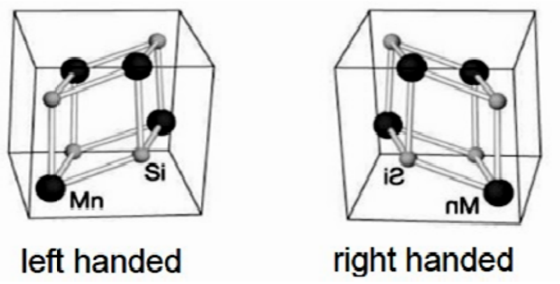

Figure 1. Unit cell of manganese silicide *MnSi*

Studies of metal deposition (especially *FeSi* and *CoSi*) on the silicon face have shown [6-10] that the formation of silicon silicide occurs on the (111) face with the highest surface energy (Table 1). The reaction on the (100) face occurs only on the oxidized surface.

Table 2 represents the thickness of the surface layer and the surface energy of the silicides of the hexagonal system.

In Table 2, the thickness $R(I)_M$ is calculated by the formula (2), and the thickness $R(I)_a$ and $R(I)_c$, as well as σa and σc are calculated by the formula (4) and (5). A noticeable anisotropy is seen both in the values of the thickness of the surface layer and in the values of the surface energy. For example, during the formation of chromium disilicide $CrSi_2$ on the (111) face in the c direction, it was found that the sizes of the islands become larger than on the (001) face (Fig. 2) [20].

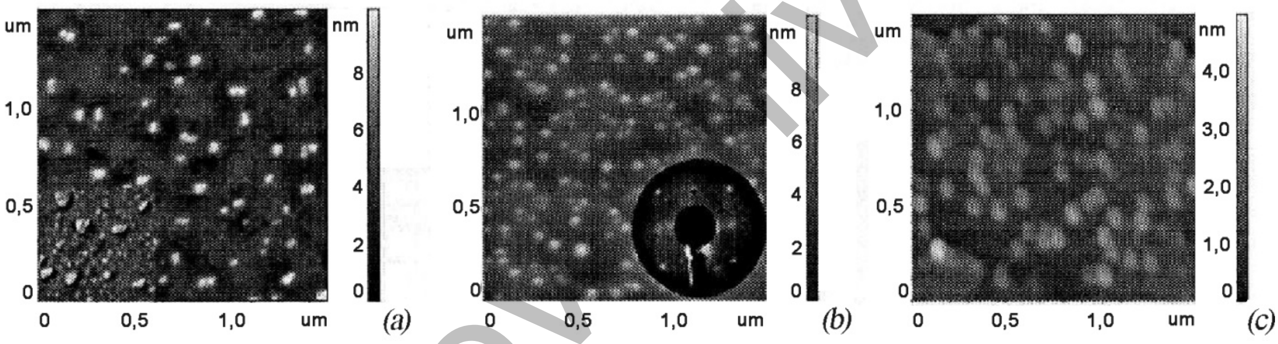

Figure 2. AFM surface of $CrSi_2$ obtained on the *Si* (001) face by reactive epitaxy (a) and solid-phase epitaxy (b) and on the *Si* (111) face obtained by reactive epitaxy (c) [20]

Table 2

Thickness of the surface layer and anisotropy of the surface energy of silicides hexagonal system

Compound	Syngonia	T_m, K	ρ, g/sm^3	M, g/mol	$R(I)_M$, nm	$R(I)_a$, nm	$R(I)_c$, nm	$σ_a$, J/m^2	$σ_c$, J/m^2
Ti_5Si_3	hexagonal	2407	4.32	322.6	17.9	7.3 (14)	22.2 (30)	0.982	2.985
$NbSi_2$	hexagonal	2223	5.66	149.08	6.30	5.9 (12)	15.4 (23)	2.082	5.434
$TaSi_2$	hexagonal	2473	9.1	237.0	6.25	5.9 (12)	15.2 (23)	2.335	6.014
$CrSi_2$	hexagonal	1823	5.0	108.167	5.19	4.7 (11)	14.0 (22)	1.651	4.918
$MoSi_2$	hexagonal	2293	6.31	152.11	5.79	1.8 (6)	26.3 (33)	0.714	10.416

This, as in the case of cubic crystals, means that the (111) face of silicon is more reactive than the other faces.

In Table 3, the thickness $R(I)_M$ is calculated by the formula (2), and the thicknesses $R(I)_a$, $R(I)_b$ and $R(I)_c$, as well as $σ_a$, $σ_b$ and $σ_c$ are calculated by the formula (4) and (5).

Table 3

Thickness of the surface layer and anisotropy of the surface energy of silicides rhombic system

Compound	Syngonia	T_m, K	$R(I)_M$, nm	$R(I)_a$, nm	$R(I)_b$, nm	$R(I)_c$, nm	σ_a, J/m^2	σ_b, J/m^2	σ_c, J/m^2
$ZrSi_2$	rhombic	1973	7.3	2.8 (8)	153.3 (108)	2.8 (8)	0.757	41.433	0.757
$HfSi_2$	rhombic	2023	7.1	2.7 (7)	166.7 (114)	2.7 (7)	0.679	47.498	0.679
$FeSi_2$	rhombic	1483	5.3	52.1 (53)	26.6 (34)	33.2 (42)	14.578	7.443	9.290
Co_2Si	rhombic	1868	4.8	11.8 (24)	2.8 (8)	19.3 (13)	4.492	1.090	7.511
Ni_2Si	rhombic	1591	4.8	19.0 (27)	6.7 (13)	2.8 (8)	6.298	2.221	0.928

Table 3 demonstrates that the $ZrSi_2$ and $HfSi_2$ crystals behave in a similar way. In the $R(I)_b$ direction, a large thickness of the surface layer is observed, leading to the formation of a dendritic structure (Fig. 3). A large surface energy is also observed on this edge.

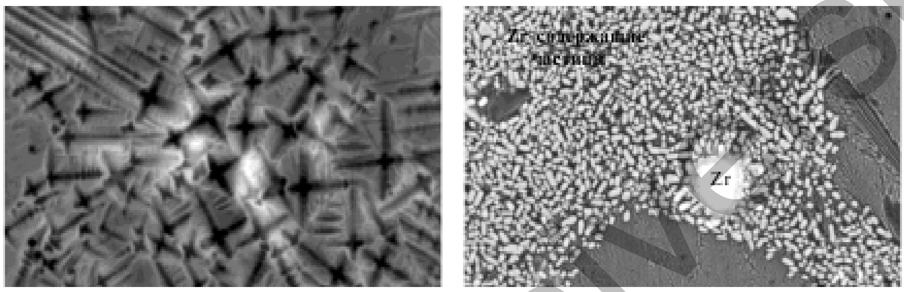

Figure 3. SEM images of the area of the dendritic structure (a) and eutectic (b) on the silicon surface during the formation of $ZrSi_2$ [16]

The thickness of the surface layer of iron disilicide $FeSi_2$ is approximately the same in all directions. This leads to spherical symmetry when grinding $FeSi_2$ in a planetary mill (Fig. 4).

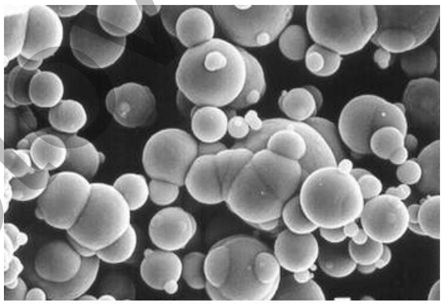

Figure 4. $FeSi_2$ in a planetary mill [21]

Figure 5 indicates an image of a nickel disilicide similar to cobalt disilicide. Image (a) describes a Ni_2Si silicide domain, where faces (b) and (c) represent the silicon silicide lattice as viewed from directions (a) and (b). It also shows the faces (101) – orange, (010) – blue, (110) – black lines. Silicon atoms Si, designated A and B at the Ni_2Si/Si interface, are shown by black spheres. Images (d) – (e) indicate layers of silicon atoms Si at the Ni_2Si/Si interface in unstressed and deformed states. The black and white atoms represent Si atoms in the Ni_2Si plane with Si end groups, and the yellow spheres represent the atoms of the Si substrate.

Overall, based on tables 1-3 it was identified that the thickness of the surface layer and specific surface energy for cubic, hexagonal and rhombic crystals have significant differences. First, the difference between the atoms of chemical elements from the periodic table and their compounds depends, first of all, on their electronic structure, which forms one or another interaction potential (such works have just begun to be studied, for example, work [22]). In this work, a pair potential was constructed, which showed that a hexagonal structure turns out to be a more favorable structure than a face-centered cubic one. Second difference between cubic, hexagonal and rhombic crystals is in their relationship with Poisson's ratio and Young's modulus, that is, on two material parameters [23-24]. Third, the thickness of the surface layer between cubic, hexagonal, and rhombic crystals also differs only in one parameter — the atomic (molar) volume of the crystal [19]. However, the analysis of all patterns still needs to be carefully analyzed.

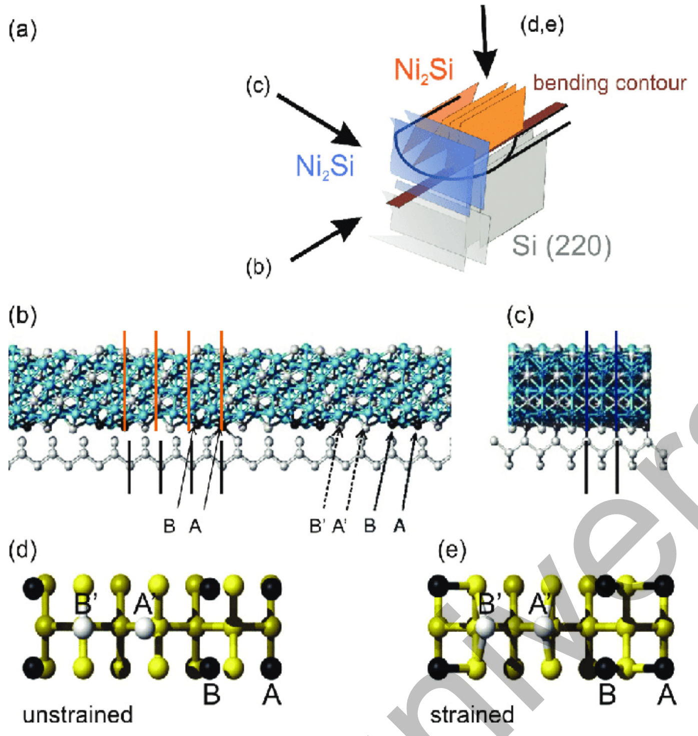

Figure 5. Nickel disilicide Ni_2Si [21]

Conclusions

In our proposed empirical model of atomically smooth metals [19] for silicon silicides of cubic, hexagonal, and rhombic systems, the thickness of the surface layer and the surface energy of the crystal faces are calculated. The average thickness of the studied crystals $R(I)_M$ does not exceed 10 nm, that is, it is a nanostructure. There is a large spread in the thicknesses in directions a, b, c of hexagonal and rhombic silicides, as well as their surface energy. This spread is associated with a change in the pair interaction potentials between atoms and a change in their Young's modulus.

Acknowledgements

The work was carried out under the program of the Ministry of Education and Science of the Republic of Kazakhstan Grants No. 0118RK000063 and No. F.0780.

References

1 Seibt M. Electronic states at dislocations and metal silicide precipitates in crystalline silicon and their role in solar cell materials / M. Seibt, R. Khalil, V. Kveder, W. Schruter // Appl. Phys. A. — 2009. — Vol. 96. — P. 235–253.

2 Zubarev E.N. Effect of working gas pressure on the formation of mixed zones in Mo/Si multilayer X-ray mirrors fabricated by magnetron sputtering / E.N. Zubarev // Advances in physical sciences. — 2011. — Vol. 181. — No. 5. — P. 491–501.

3 Глушков В.Л. Характеристики поверхности щелочных металлов с учетом дискретности кристаллической решетки и фриделевских осцилляций электронной плотности / В.Л. Глушков, О.С Еркович // Вестн. МГТУ им. Н.Э. Баумана. Сер. Естественные науки. — 2017. — Вып. 73. — № 4. — С. 75–89.

4 Shebzukhova I.G. Anisotropy of surface energy and electron work function IIB of metals / I.G. Shebzukhova, L.P. Arefieva // Physical and Chemical Aspects of Study of Clusters Nanostructures and Nanomaterials. — 2020. — No. 12. — P. 319.

5 Bokarev V.P. Anisotropy of physicochemical properties of single-crystal surfaces / V.P. Bokarev, G.Ya. Krasnikov // Electronic technology. Series 3. Microelectronics. — 2016. — No. 4 (164). — P. 25–32.

6 Gomoyunova M.V. Formation of ultrathin layers of iron silicides on the surface of monocrystalline silicon / M.V. Gomoyunova, I.I. Pronin, D.E. Malygin, N.R. Gall, D.V. Vyalikh, S.L. Molodtsov // Surf. Sci. — 2006. — Vol. 600. — P. 2449–2457.

7 Tsay J.S. Microscopic interfacial structures and magnetic properties of ultrathin Co/Si (111) Co/Si (111) films / J.S. Tsay, T.Y. Fu, M.H. Lin, C.S. Yang, Y.D. Yao // Appl. Phys. Lett. — 2006. — Vol. 88. — P. 102–113.

8 Mühlbauer S. Skyrmion lattice in a chirial magnet / S. Mühlbauer, B. Binz, F. Jonietz, C. Pfleiderer, A. Rosch, A. Neubauer, R. Georgii, P. Boeni // Science. — 2009. — Vol. 323. — P. 915–928.

9 Gomoyunova M.V. Formation of manganese silicides on the Si (111) 7x7 surface / M.V. Gomoyunova, G.S. Grebenyuk, I.I. Pronin, B.V. Senkovsky, D.V. Vyalykh // Solid State Physics. — 2015. — Vol. 57. — No. 3. — P. 609–618.

10 Galkin K.N. Electrical properties of two-dimensional iron layers in ordered phases Si (111) 7x7 and Si (111) 2x2-fe / K.N. Galkin, S.A. Dotsenko, N.G. Galkin // Chemical Physics and Mesoscopy. — 2009. — Vol. 11. — No. 3. — P. 334–342.

11 Grigorenko S.G. Titanium intermetallic compounds. Features, properties, application (Review) / S.G. Grigorenko, G.M. Grigorenko, O.M. Zadorozhnyuk // Modern electrometallurgy. — 2017. — № 3 (128). — P. 51–63.

12 Afonin N.N. Properties of thin films based on iron oxide and titanium formed on single-crystal silicon / N.N. Afonin, V.A. Logacheva, Yu.S. Shramchenko, A.M. Khoviv // Journal of Inorganic Chemistry. — 2011. — Vol. 56. — No. 5. — 821–832.

13 Sotiriou G.A. Janus-Like Plasmonic-Magnetic Nanoparticles / G.A. Sotiriou, A.M. Hir, P.Y. Lozach, A. Teleki, F. Krumeich, S.E. Pratsinis // Chem. Mater. — 2011. — Vol. 23 (7). — P. 1985–1993.

14 Соловьев Я.А. Влияние температуры быстрой термической обработки на электрофизические свойства пленок никеля на кремнии / Я.А. Соловьев, В.А. Пилипенко // Докл. БГУИР. — 2020. — № 18 (1). — С. 81–88.

15 Jiang D.E. Prediction of strong adhesion at the MoSi$_2$/Fe interface / D.E. Jiang, A. Emily, E.A. Carter // Acta Materialia. — 2015. — Vol. 53. — P. 4489–4497.

16 Angles V.V. Synthesis of multicomponent nanocrystalline coatings based on titanium nitride in arc low-pressure discharges / V.V. Angles, N.N. Koval, Yu.F. Ivanov, Yu.A. Petukhov, A.V. Kalin, A.D. Teresov // Surface. X-ray, synchrotron and neutron research. — 2013. — No. 3. — P. 57–64.

17 Filonov A.B. Semiconductor silicides: properties and prospects of application / A.B. Filonov, V.E. Borisenko, W. Henrion, H. Lange // Journal of Luminescence. — 1999. — Vol. 80. — 479–493.

18 Кичигин В.И. Исследование механизма катодных процессов на силицидах кобальта методом электрохимической импедансной спектроскопии / В.И. Кичигин, А.Б. Шеин // Вестн. ТГУ. Сер. Химия. — 2013. — Вып. 18. — № 5. — С. 2209–2215.

19 Yurov V.M. Surface layer thickness, surface energy, and atomic volume of an element / V.M. Yurov, S.A. Guchenko, V.C. Laurinas // Physical and chemical aspects of studying clusters, nanostructures and nanomaterials. — 2018. — No. 10. — P. 691–701.

20 Galkin N.G. Silicon-silicide quasi-zero dimensional heterostructures for silicon based photonics, opto- and thermoelectronics / N.G. Galkin, D.L. Goroshko, E.A. Chusovitin, K.N. Galkin // Physics Status Solidi C. — 2013. — Vol. 10. — P. 1670–1683.

21 Alberti A. Role of the early stages of Ni-Si interaction on the structural properties of the reaction products / A. Alberti, A. La Magna // J. Appl. Phys. — 2013. — Vol. 114. — P. 121–301.

22 Podolskaya E.A. Description of the geometry of crystals with a hexagonal close-packed structure based on pair interaction potentials / E.A. Podolskaya, A.M. Krivtsov // Solid State Physics. — 2012. — Vol. 54. — 1327–1334.

23 Гольдштейн Р.В. Ауксетическая механика кристаллических материалов / Р.В. Гольдштейн, В.А. Городцов, Д.С. Лисовенко // Механика твердого тела. — 2010. — № 4. — С. 43–54.

24 Yurov V.M. Structural phase transition in surface layer of metals / V.M. Yurov, S.A. Guchenko, V.Ch. Laurinas, O.N. Zavatskaya // Bulletin of the Karagandy University – Physics Series. — 2019. — № 1 (93). — P. 50–60.

В.М. Юров, В.И. Гончаренко, В.С. Олешко, Қ.М. Маханов

Кейбір металдардың силицидтерінің беттік энергиясының анизотропиясы

Мақалада қатты дене бетінің эмпирикалық моделі ұсынылған. Элементтің атомдық көлемі немесе оның қосылыстары беттік қабаттың қалыңдығы бір параметр арқылы өрнектелген. Сонымен қатар химиялық элементтің немесе кристалдың балқу температурасы беттік энергияда бір параметр арқылы өрнектелді. Модельде кристалдың әр қыры үшін беттік қабаттың қалыңдығы мен беттік энергияны есептеуге мүмкіндік беретін теңдеулер ұсынылған. Мысал ретінде кубты, гексогональды және ромбтық сингониялы кристалдық құрылымға ие кейбір металдардың силицидтері үшін осы шамалардың есептеулері жасалды. Кубтық силицидтерде беттік қабаттың қалыңдығы 3–9 нм, ал моноқабаттар саны 7–16 құрайды. Кремний беттеріне металды тұндыру үрдісін зерттеулер көрсеткендей, кремний силицидінің қалыптасуы, беттік энергиясы ең жоғары болатын (111) қырда түзіледі. (100) қырында реакция тек тотыққан бетінде жүреді. Гексагональды силицидтерде, беттік қабаттың қалыңдықтарының шамаларында да, сондай–ақ, беттік энергия шамаларында да елеулі анизотропия байқалады. Мысалы, хром-дисилицидін (111) қырында қалыптастырғанда, *c* бағытындағы аралдардың өлшемдері (001) қырдағыға қарағанда үлкен болатыны байқалған. Авторлар мақалада кубтық, гексогональдық және ромбтәрізді кристалдар үшін беттік қабаттың қалыңдығы мен беттік меншікті энергияның бір–бірінен едәуір айырмашылығы бар екендігін көрсеткен. Айырмашылық неде? Біріншіден, периодтық кестедегі химиялық элементтердің атомдарымен олардың қосындыларының арасындағы айырмашылық, ең алдымен олардың өзара әрекеттесу потенциалын құрайтын электрондық құрылымына байланысты. Екіншіден, кубтық, гексогональдық және ромбтәрізді кристалдар арасындағы айырмашылық олардың Пуассон коэффициентімен және

Юнг модулімен байланыстарына қатысты, демек, олар екі материалдық параметрден. Үшіншіден, кубтық, гексогональдық және ромбтәрізді кристалдар арасындағы беттік қабаттың қалыңдығы да тек бір параметрмен — кристалдың атомдық (молярлық) көлемімен ерекшеленеді. Дегенмен, барлық заңдылықтарды талдау нәтижелері зерттеу жұмыстарын әлі де мұқият орындауды қажет етеді.

Кілт сөздер: металл силициді, беттік энергия, беттік қабаттың қалыңдығы, қатты дене, химиялық элемент, кристалл, беттік қабат, Пуассон коэффициенті, Юнг модулі.

В.М. Юров, В.И. Гончаренко, В.С. Олешко, К.М. Маханов

Анизотропия поверхностной энергии силицидов некоторых металлов

В статье предложена эмпирическая модель поверхности твердого тела. Толщина поверхностного слоя показана через один параметр — атомный объем элемента или его соединений. Поверхностная энергия выражена также через один параметр — температуру плавления химического элемента или кристалла. В модели предложены уравнения, которые позволяют вычислить толщину поверхностного слоя и поверхностную энергию для каждой грани кристалла. В качестве примера сделаны расчеты этих величин для силицидов некоторых металлов, имеющих кристаллическую структуру кубической, гексагональной и ромбической сингонии. У кубических силицидов толщина поверхностного слоя составляет 3–9 нм, а число монослоев — 7–16. Исследования нанесения металла на грани кремния показали, что формирование силицида кремния происходит на грани (111), обладающей наибольшей поверхностной энергией. Реакция на грани (100) наблюдается только на окисленной поверхности. У гексагональных силицидов видна заметная анизотропия, как в значениях толщин поверхностного слоя, так и в величинах поверхностной энергии. Например, при формировании дисилицида хрома на грани (111) в направлении *c* обнаружено, что размеры островков становятся больше, чем на грани (001). Авторами показано, что толщина поверхностного слоя и удельная поверхностная энергия для кубических, гексагональных и ромбических кристаллов существенно от них отличаются. В чем заключается различие? Во-первых, отличие между атомами химических элементов из периодической таблицы и их соединениями зависит, прежде всего, от их электронного строения, формирующего тот или иной потенциал взаимодействия. Во-вторых, разница между кубическими, гексагональными и ромбическими кристаллами состоит в их связи с коэффициентом Пуассона и модулем Юнга, то есть зависит от двух материальных параметров. В-третьих, толщина поверхностного слоя между кубическими, гексагональными и ромбическими кристаллами также отличается только одним параметром — атомным (молярным) объемом кристалла. Однако анализ всех закономерностей нужно тщательно перепроверить.

Ключевые слова: силицид металла, поверхностная энергия, толщина поверхностного слоя, твердое тело, химический элемент, кристалл, поверхностный слой, коэффициент Пуассона, модуль Юнга.

References

1 Seibt, M., Khalil, R., Kveder, V., & Schruter W. (2009). Electronic states at dislocations and metal silicide precipitates in crystalline silicon and their role in solar cell materials. *Appl. Phys.A.,* 96, 235–253.

2 Zubarev, E.N. (2011). Effect of working gas pressure on the formation of mixed zones in Mo/Si multilayer X-ray mirrors fabricated by magnetron sputtering. *Advances in physical sciences*, 181, 5, 491–501.

3 Glushkov, V.L. & Erkovich, O.S. (2017). Kharakteristiki poverkhnosti shchelochnykh metallov s uchetom diskretnosti kristallicheskoi reshetki i fridelevskikh ostsilliatsii elektronnoi plotnosti [Characteristics of the surface of alkali metals taking into account the discreteness of the crystal lattice and Friedel oscillations of the electron density]. *Vestnik MGTU imeni N.E. Baumana. Seriia Estestvennye nauki — Bulletin of N.E. Bauman University. Series Natural Sciences, Vol. 73, 4*, 75–89 [in Russian].

4 Shebzukhova, I.G. & Arefieva, L.P. (2020). Anisotropy of surface energy and electron work function IIB of metals. *Physicochemical aspects of studying clusters, nanostructures and nanomaterials*, 12, 319.

5 Bokarev, V.P., & Krasnikov, G.Ya. (2016). Anisotropy of physicochemical properties of single-crystal surfaces. *Electronic technology. Series 3. Microelectronics*, 4 (164), 25–32.

6 Gomoyunova, M.V., Pronin, I.I., Malygin, D.E, Gall, N.R., Vyalikh, D.V., & Molodtsov, S.L. (2006). Formation of ultrathin layers of iron silicides on the surface of monocrystalline silicon. *Surf. Sci.,* 600, 2449–2457.

7 Tsay, J.S., Fu, T.Y., Lin, M.H., Yang, C.S., & Yao, Y.D. (2006). Microscopic interfacial structures and magnetic properties of ultrathin Co/Si (111) Co/Si (111) films. *Appl. Phys. Lett.,* 88, P. 102–113.

8 Mühlbauer, S., Binz, B., Jonietz, F., Pfleiderer, C., Rosch, A., & Neubauer, A., et al. (2009). Skyrmion lattice in a chirial magnet. *Science*, 323, 915–928.

9 Gomoyunova, M.V., Grebenyuk, G.S., Pronin, I.I., Senkovsky, B.V., & Vyalykh, D.V. (2015). Formation of manganese silicides on the Si (111) 7x7 surface. *Solid State Physics*, 57, 3, 609–618.

10 Galkin, K.N., Dotsenko, S.A. & Galkin, N.G. (2009). Electrical properties of two-dimensional iron layers in ordered phases Si (111) 7x7 and Si (111) 2x2-fe. *Chemical Physics and Mesoscopy*, 11, 3, 334–342.

11 Grigorenko, S.G., Grigorenko, G.M. & Zadorozhnyuk, O.M. (2017). Titanium intermetallic compounds. Features, properties, application (Review). *Modern electrometallurgy*, *3* (128), 51–63.

12 Afonin, N.N., Logacheva, V.A., Shramchenko, Yu.S., & Khoviv, A.M. (2011). Properties of thin films based on iron oxide and titanium formed on single-crystal silicon. *Journal of Inorganic Chemistry*, 56, 5, 821–832.

13 Sotiriou, G.A., Hir, A.M., Lozach, P.Y., Teleki, A., Krumeich, F., & Pratsinis, S.E. (2011). Janus-Like Plasmonic-Magnetic Nanoparticles. *Chem. Mater.*, 23 (7), 1985–1993.

14 Soloviev, Ya.A., & Pilipenko, V.A. (2020). Vliianie temperatury bystroi termicheskoi obrabotki na elektrofizicheskie svoistva plenok nikelia na kremnii [Influence of conditions of rapid heat treatment on the electrophysical properties of thin chromium films on silicon]. *Doklady BGUI — Reports of BSUIR*, *18(1),* 81–88 [in Russian].

15 Jiang, D.E., Emily, A. & Carter, E.A. (2005). Prediction of strong adhesion at the $MoSi_2$/Fe interface. *Acta Materialia*, 53, 4489–4497.

16 Angles, V.V., Koval, N.N., Ivanov, Yu.F., Petukhov, Yu.A., Kalin, A.V., & Teresov, A.D. (2013). Synthesis of multicomponent nanocrystalline coatings based on titanium nitride in arc low-pressure discharges. *Surface. X-ray, synchrotron and neutron research*, 3, 57–64.

17 Filonov, A.B., Borisenko, V.E., Henrion, W., & Lange, H. (1999). Semiconductor silicides: properties and prospects of application. *Journal of Luminescence*, 80, 479–493.

18 Kichigin, V.I. & Shein, A.B. (2013). Issledovanie mekhanizma katodnykh protsessov na silitsidakh kobalta metodom elektrokhimicheskoi impedansnoi spektroskopii [Study of the mechanism of cathodic processes on cobalt silicides by the method of electrochemical impedance spectroscopy]. *Vestnik TGU. Khimiia — Bulletin of TSU. Chemistry*, *Vol. 18, 5,* 2209–2215 [in Russian].

19 Yurov, V.M, Guchenko, S.A. & Laurinas, V.C. (2018). Surface layer thickness, surface energy, and atomic volume of an element. *Physical and chemical aspects of studying clusters, nanostructures and nanomaterials*, 10, 691–701.

20 Galkin, N.G., Goroshko, D.L., Chusovitin, E.A., & Galkin, K.N. (2013). Silicon-silicide quasi-zero dimensional heterostructures for silicon based photonics, opto- and thermoelectronics. *Physica Status Solidi C.,* 10, 1670–1683.

21 Alberti, A. & La Magna, A. (2013). Role of the early stages of Ni-Si interaction on the structural properties of the reaction products. *J. Appl. Phys.*, 114, 121–301.

22 Podolskaya, E.A. & Krivtsov, A.M. (2012). Description of the geometry of crystals with a hexagonal close-packed structure based on pair interaction potentials. *Solid State Physics*, 54, 1327–1334.

23 Goldstein, R.V., Gorodtsov, V.A. & Lisovenko, D.S. (2010). Aukseticheskaia mekhanika kristallicheskikh materialov [Auxetic Mechanics of Crystalline Materials]. *Mekhanika tverdogo tela — Mechanics of Solids, 4,* 43–54 [in Russian].

24 Yurov, V.M., Guchenko, S.A., Laurinas, V.Ch., & Zavatskaya, O.N. (2019). Structural phase transition in surface layer of metals. *Bulletin of the Karagandy University – Physics*, 1 (93), 50–60.